



HAL
open science

Impact of acoustic airflow nebulization on intrasinus drug deposition of a human plastinated nasal cast: New insights into the mechanisms involved

Marc Durand, Jérémie Pourchez, Gérald Aubert, Sandrine Le Guellec,
Laurent Navarro, Valérie Forest, Philippe Rusch, Michèle Cottier

► **To cite this version:**

Marc Durand, Jérémie Pourchez, Gérald Aubert, Sandrine Le Guellec, Laurent Navarro, et al.. Impact of acoustic airflow nebulization on intrasinus drug deposition of a human plastinated nasal cast: New insights into the mechanisms involved. *International Journal of Pharmacy*, 2011, 421 (1), pp.63-71. 10.1016/j.ijpharm.2011.09.023 . hal-00640705

HAL Id: hal-00640705

<https://hal.science/hal-00640705>

Submitted on 14 Nov 2011

HAL is a multi-disciplinary open access archive for the deposit and dissemination of scientific research documents, whether they are published or not. The documents may come from teaching and research institutions in France or abroad, or from public or private research centers.

L'archive ouverte pluridisciplinaire **HAL**, est destinée au dépôt et à la diffusion de documents scientifiques de niveau recherche, publiés ou non, émanant des établissements d'enseignement et de recherche français ou étrangers, des laboratoires publics ou privés.

Impact of Acoustic Airflow Nebulization on Intranasal Drug Deposition of a Human Plastinated Nasal Cast: New Insights into the Mechanisms involved

Marc DURAND^{1,2,3}, Jérémie POURCHEZ^{2,3,4*}, Gérald AUBERT⁵, Sandrine LE GUELLEC^{6,7}, Laurent NAVARRO^{3,4}, Valérie FOREST^{2,3,4}, Philippe RUSCH^{2,3,5,8,9}, Michèle COTTIER^{2,3,5,8,9}

¹ Centre Hospitalier Emile Roux, F-43012, Le Puy en Velay, France

² LINA, Laboratoire Interdisciplinaire d'étude des Nanoparticules Aérosolisées, EA 4624, F-42023, Saint-Etienne, France

³ SFR IFRESIS, F-42023, Saint-Etienne, France

⁴ Ecole Nationale Supérieure des Mines de Saint-Etienne, Centre Ingénierie et Santé, F-42023, Saint-Etienne, France

⁵ CHU de Saint-Etienne, F-42055, Saint-Etienne, France

⁶ DTF-Aerodrug, Faculté de médecine, F-37032, Tours, France

⁷ INSERM-U618, Faculté de Médecine, F-37032, Tours, France

⁸ Université Jean Monnet, Faculté de Médecine, F-42023, Saint-Etienne, France

⁹ Université de Lyon, F-42023, Saint-Etienne, France

* Corresponding author: Tel: (+33) 4 77 42 01 80; Fax: (+33) 4 77 49 96 94;
E-mail address: pourchez@emse.fr

1 **ABSTRACT**

2 *Purpose:* The impact of 100 Hertz (Hz) acoustic frequency airflow on sinus drug deposition
3 of aerosols was investigated using a human plastinated nasal cast. The influence of drug
4 concentration and endonasal anatomical features on the sinus deposition enhanced by the 100
5 Hz acoustic airflow was also examined.

6 *Methods:* Plastinated models were anatomically, geometrically and aerodynamically validated
7 (endoscopy, CT scans, acoustic rhinometry and rhinomanometry). Using the gentamicin as a
8 marker, 286 experiments of aerosol deposition were performed. Changes of airborne particles
9 metrology produced under different nebulization conditions (100 Hz acoustic airflow and
10 gentamicin concentration) were also examined.

11 *Results:* Aerodynamic and geometric investigations highlighted a global behaviour of
12 plastinated models in perfect accordance with a nasal decongested healthy subject. The results
13 of intrasinus drug deposition clearly demonstrated that the aerosols can penetrate into the
14 maxillary sinuses. The 100 Hz acoustic airflow led to increase the deposition of drug into the
15 maxillary sinuses by a factor 2 to 3 depending on the nebulization conditions. A differential
16 intrasinus deposition of active substance depending on maxillary ostium anatomical features
17 and drug concentration was emphasized.

18 *Conclusion:* The existence of a specific transport mechanism of penetration of nebulized
19 particles delivered with acoustic airflow was proposed.

20 **Keywords:** acoustic airflow, aerosol therapy, drug deposition, plastination, maxillary sinus.

21

22

23

24

25

26 **1. Introduction**

27 Rhinosinusitis is a significant and increasing health problem which results in a large financial
28 burden on society (Fokkens *et al.*, 2007). Due to the inflammation of the nasal mucosa or
29 impaired mucociliary clearance, the blockage of sinus drainage leads to the creation of a
30 favourable environment for sinusitis. Indeed, under these conditions bacteria and viruses
31 cannot be removed by secretions drainage and may proliferate. Targeting delivery of
32 nebulized antibiotics into the maxillary sinuses, the sites of infection, could improve clinical
33 outcomes in patients with chronic rhinosinusitis. Thus, nasal drug delivery by nebulization is
34 widely used in sinus disorders, because of its safety and convenience and due to its
35 advantages as a painless therapy. Topical delivery of antimicrobial drugs for treatment of
36 rhinosinusitis also brings intuitive advantages over systemic therapy. It minimizes the risk of
37 systemic side effects, the development of antibiotic resistance in non targeted areas and
38 allows a high topical drug concentration deposition with a minimal systemic adsorption.
39 However the nebulization conditions to facilitate penetration of aerosols into the sinus cavities
40 are not well-established. The practice of aerosol therapy to treat rhinosinusitis has not been
41 studied thoroughly, despite few works have shown clinical benefit (Vaughan *et al.*, 2002).
42 The main issue is that it remains very difficult to demonstrate an effective penetration of
43 aerosolized drugs into paranasal sinuses which are poorly ventilated hollow cavities due to
44 anatomical features. The maxillary sinuses communicate with the nasal fossa via narrow
45 ducts: the maxillary ostia (about 1-5 mm in diameter; 10-15 mm in length) (Tarhan *et al.*,
46 2005). However, some *in vivo* and *in vitro* studies have demonstrated that aerosolized
47 particles can be deposited into paranasal sinuses but always at low concentrations (Hyo *et al.*,
48 1989; Saijo *et al.*, 2004; Hilton *et al.*, 2008; Durand *et al.*, 2001). These studies highlighted
49 that the three main factors affecting the aerosol deposition into the maxillary sinuses are: the
50 diameter/length of the maxillary ostium, the pressure/rate of the aerosol, and finally the
51 airborne particle size. All things considered, a better understanding of ventilation and drug

52 delivery to the maxillary sinuses is required to more accurately define the relevance of nasal
53 drug delivery for treatment of rhinosinusitis despite the fact it is widely used by the clinicians.
54 To enhance the penetration of nebulized particles into badly-ventilated areas (*i.e.* sinuses in
55 healthy subject) or non-ventilated areas (*i.e.* sinuses in patients with sinus diseases), a
56 pressure gradient generated by a acoustic airflow can be added to a usual jet nebulizer
57 (Guillerm *et al.*, 1959). Few literature citations consider the possible increase in value when
58 an acoustic pressure wave is added to aerosol. Vecellio *et al.* recently demonstrated that,
59 using a nasal sonic jet nebulizer loaded with ^{99m}Tc -DTPA in seven healthy male non-
60 smoking volunteers, aerosol deposition in the nasal cavity was $73 \pm 10\%$ (% of aerosol
61 deposited into the airways) (Vecellio *et al.*, 2011). They also highlighted that $5 \pm 2\%$ of the
62 total activity deposited into the nasal cavity was deposited in the maxillary sinuses. Moeller *et*
63 *al.* showed in healthy volunteers a significant increased of ^{81m}Kr gas ventilation of the
64 paranasal sinuses using pulsating airflow (Moeller *et al.*, 2008). These authors also showed
65 that $6 \pm 2\%$ of the total nose deposition reached the sinuses with pulsating aerosol delivery
66 although less than 1% of this dose penetrated into the sinuses using a nasal pump spray
67 (Moeller *et al.*, 2010). Similarly, Maniscalco *et al.* demonstrated that a acoustic airflow
68 increased the delivery of an aerosolised drug into the paranasal sinuses (Maniscalco *et al.*,
69 2006). But the gain of intrasinus drug deposition brought by the use of acoustic airflow is
70 neither well-established nor well-understood. Moreover, the underlying particle transport
71 mechanism into the sinuses remains misunderstood.

72 Three main families of human nasal casts can be distinguished to study aerosol deposition:
73 “pipe models” (Moeller *et al.*, 2008; Maniscalco *et al.*, 2006; Cakmak *et al.*, 2003), plastic
74 replicas (Schreck *et al.*, 1993; Kelly *et al.*, 2000) and models obtained from cadavers (Hilton
75 *et al.*, 2008). Unfortunately, the usual experimental casts present some drawbacks or specific
76 restrictions: “pipe models” may not adequately mimic the anatomy of the human cavity,
77 plastic replicas can suffer from a lack of thin anatomical details (such as the maxillary ostium

78 morphology), and models from cadavers raise issues of time stability and biosecurity. Thus, a
79 concept of human plastinated nasal cast without any tissue retraction phenomenon was
80 proposed. Plastination permits the preservation of anatomical specimens in a physical state
81 approaching that of the living condition. This technique was introduced by Dr. Gunther von
82 Hagens in late 1970s (von Hagens, 1979). The plastination consists in replacing water and
83 lipids in biological tissue by curable polymers. The advantages of plastinated nasal specimens
84 are numerous: anatomical and aerodynamic behaviour close to *in vivo*, huge time-stability,
85 water-washability, accessibility of the maxillary sinuses, easy handling, dry odourless,
86 biologically safe and transportable without constraints.

87 This study aims at investigating the deposition of aerosols in the maxillary sinuses of a
88 plastinated human nasal cast presenting dissimilar anatomical features of ostia, with and
89 without acoustic airflow. The main purpose of this work was to highlight the influence of the
90 100 Hz acoustic frequency on the sinus drug deposition. To improve our understanding of the
91 mechanisms involved, the gain of efficiency brought by the 100 Hz acoustic frequency was
92 also evaluated depending on the gentamicin concentration initially introduced into the
93 nebulizer and the maxillary ostium anatomical features. Thus, we successively performed
94 anatomical and aerodynamic characterisations of the plastinated nasal cast, and studied the
95 metrology of the aerosol (particle size and aerosol output rate) and the acoustic
96 characterization of the 100 Hz acoustic frequency. Then we conducted 286 experiments of
97 drug deposition into the maxillary sinuses using various nebulization conditions.

98

99 **2. Materials and methods**

100 *2.1 Elaboration of plastinated nasal model*

101 A specific plastination technique of cephalic extremities was developed in our laboratory over
102 the last 10 years in order to obtain nasal casts without any tissue retraction and dedicated to
103 functional studies (e.g. aerodynamic and aerosol deposition studies) (Durand *et al.*, 2001;

104 Croce *et al.*, 2006). In this paper, we focus on a plastinated specimen (Figure 1) obtained from
105 a deceased man who left his body to the Saint-Etienne Anatomy Laboratory. The plastination
106 process consists in different successive steps: anatomical sampling, section, fixation,
107 dissection, dehydration and degreasing, polymer forced impregnation in a vacuum, and then,
108 curing and polymerization. All these steps were recently described in details in a form that a
109 lab scientist could follow the procedure and generate an identical cast (Durand *et al.*, 2011).
110 Last, a specific lateral-paramedian section of the plastinated head was performed to open an
111 exterior free access to the maxillary sinuses via the cheekbone (Figure 1). Maxillary volumes
112 and aerodynamic behaviour of the model were nevertheless kept normal. This original
113 opening allowed the collection and so the quantification of the active drug deposited into
114 maxillary sinuses during aerosol studies. Technically, two removable plexiglass plates were
115 used to hermetically close (“closed position” shown in Figure 2 step1), or not (“open
116 position” shown in figure1B) the maxillary exterior opening during nebulization experiments
117 and aerodynamic measures.

118 Legal and ethical principles were strictly respected during the elaboration of plastinated nasal
119 model. Body donation to science authorizes in France a university to use a cadaver for
120 teaching and research activities. The different steps of body donation to science are not
121 governed by the French laws of bioethics, but by several legal and administrative texts.
122 Before to use a cadaver obtained by donation, an authorization was obtained in which is
123 clearly defines the usages for research and teaching. The legal’s rules of anonymity were also
124 complied and the donors were informed on the use of their donation. The respect of the
125 donors and their families remains a key point of the administration ability to receive these
126 donations. For all these reasons, the French Research Ethics committees do not have a legal’s
127 rules to approve the individual research on a cadaver. However the respect of good practices
128 is frequently checked and valued.

129

2.2 Anatomical and aerodynamic characterization of the plastinated nasal cast

The objective of the characterization work was to evaluate the reliability of nasal cavity geometry and airflow resistance of the plastinated specimen compared to *in vivo* data. The methodologies used to anatomically, geometrically and aerodynamically characterize the plastinated nasal cast were recently described in details (Durand et al., 2011). A clinical anatomy study was firstly carried out using CT scans and endoscopy observations. These techniques were performed on the plastinated model in order to evaluate the preservation of mucosa in the cast (especially in the middle turbinate area) as well as to precisely define the geometrical features of the maxillary ostia. The geometry of nasal cavities was also characterized using acoustic rhinometry. This method is frequently used to determine *in vivo* the nasal cross-sectional areas through acoustics reflexion. Each nasal fossa of the plastinated specimen was separately examined leading to the characterization of the first six centimetres corresponding to the longitudinal area from the tip of the nostril to the middle meatus region. As a matter of fact, beyond the sinus ostium region, the acoustic rhinometry overestimates cross-sectional area and provide no quantitative data for sinus volume or ostium size (Tarhan *et al.*, 2005).

Aerodynamic assessments were also performed using rhinomanometry providing an objective quantification of nasal airway resistance. Indeed, rhinomanometry is a well-established and reliable technique that measures nasal patency in terms of nasal airflow and resistance to airflow. The measured pressure–flow relationship reflects the functional status of the nasal airway. We examined separately the resistance of each nasal cavity (in “closed position”) while the opposite nostril was occluded. Moreover, and for the first time, the serial resistance of both nasal cavity and ostium was also measured. For example, to measure the airflow resistance of ostium and nasal cavity on the right side, both nostrils were occluded, and right sinus cavity was kept in “open position” while the left sinus cavity in “closed position”. These

155 original and novel data provide some very important information on the impact of the ostium
156 morphology on airflow resistance to enter the maxillary sinus cavity.

157

158 *2.3 Nebulization system*

159 The nebulization system, including an Atomisor NL11SN jet nebulizer associated with an
160 AOLH[®] air source compressor (Diffusion Technique Française, DTF Medical, Saint-Etienne,
161 France), can produced a “sonic aerosol” by adding a 100 Hz acoustic frequency during
162 aerosol production. The acoustic frequency was continuously emitted since a vibrating
163 capsule in the compressor (AS[®] sonic generator, 110 Volts, DTF Medical, Saint-Etienne,
164 France) and conducted through a 5 mm in width and 1-m in length tube (8.5 mm inside
165 diameter) to the nebulizer outlet. Nebulizations were performed according to two options
166 operating mode of the compressor/sonic generator: the classic mode without addition of the
167 100 Hz acoustic frequency, and the sonic mode with addition of the 100 Hz acoustic
168 frequency. The nebulizer NL11SN was equiped with a nasal plug (C28 medium size,
169 Diffusion Technique Française, DTF Medical, Saint-Etienne, France) purchased by the
170 manufacturer and usually used in clinical practice. This nasal plug ensured the interface
171 connection between nebulizer and the plastinated model’s nostrils. Depending on the
172 nebulization experiment, the NL11SN was filled either with 4 mL of a gentamicin solution, or
173 with 4 mL of NaF 2.5% solution. The nebulizer operates at a flow rate of 8 L.min⁻¹.

174

175 *2.4 Acoustic signal of the acoustic airflow*

176 The acoustic pressure waves added to the aerosol during its production by the sonic nebulizer
177 NL11SN was characterized for a better understanding of its influence on aerosolized particles
178 deposition in the maxillary sinuses. The acoustic signal coming out of the NL11SN has been
179 characterized by a usual signal processing methodology, using a digital sound level meter (AZ
180 Instrument) which measures the maximum acoustic pressure level. The measurements have

181 been performed in free field (the distance from the walls was high enough to not influence the
182 signal's behaviour and its frequency content) at exactly 1 cm of the output pipe. Besides the
183 determination of the frequency components of the signal (fundamental amplitude and
184 potential harmonics) a spectral analysis using the Fourier transform was used.

185

186 2.5 Aerosol metrology

187 The aim of the metrology study was to determine the impact of the 100 Hz acoustic frequency
188 on the aerosol output and the particle size. All metrology experiments are summarized in
189 Table 1. The output of gentamicin aerosol was measured simulating respiration with a
190 sinusoidal pump and collecting aerosol on a filter. An absolute filter (Inhalation Filter Pad,
191 Pari GmbH, Germany) was interposed between the nebulizer system and the respiratory pump
192 (Compas2, Pari GmbH, Germany) which was regulated according to standard NF EN 13544-
193 1 (*i.e.* Sinus pattern - Tidal Volume of 500 mL - 15 breath/min - Inspiration:Expiration = 1:1).
194 The equipments and fluids were stabilized at ambient conditions before use. The nebulizer
195 system was connected to its associated compressor. Gentamicin was introduced into the
196 nebulizer. The respiratory pump and compressor were turned on. Nebulization time was
197 limited to 10 minutes. The amount of gentamicin collected by the filter was determined by a
198 residual gravimetric method based on weighing dry filters (Vecellio *et al.*, 2004). The output
199 fraction was obtained by calculating the ratio between the amount of gentamicin collected on
200 the filter and the amount of gentamicin initially introduced into the nebulizer.

201 Aerosol particle sizing was defined in terms of Mass Median Aerodynamic Diameter
202 (MMAD). The MMAD was assessed using cascade impaction according to two
203 complementary approaches using the NGI (Next Generation pharmaceutical Impactor, Copley
204 Scientific, USA) and the ELPI (Electrical Low Pressure Impactor, Dekati Ltd, Finland). In
205 cascade impactors, the aerosolized particles are impacted on different stages depending on
206 their inertia related to their aerodynamic diameter. These devices allow simultaneous measure

207 of the aerodynamic size and of the mass of active drug according to the different size ranges.
208 The metrology was conducted either with sodium fluoride (NaF; 2.5% wt; 4 mL) a chemical
209 tracer recommended by European standard procedure (NF EN 13544-1), but also with
210 gentamicin (40 and 80 mg.mL⁻¹; 4 mL). Unlike the ELPI which was originally designed for
211 industrial and environmental aerosols, the NGI was specifically designed for pharmaceutical
212 aerosols and has been included in the British Pharmacopoeia as a test method for the
213 measurement of aerodynamic particle size distribution (Marple et al., 2004). Thus the NGI
214 was preferentially used for metrology experiments using gentamicin, because this cascade
215 impactor was specifically designed to meet the requirements of the US and European
216 pharmacopeia. The ELPI was preferentially used for metrology experiments using NaF, for its
217 ability to characterize particle size at a nanometric range, which could be helpful if the
218 acoustic airflow decreases the aerosol particle size.

219 The ELPI allows the collection of nebulized particles from 7 nm to 10 µm into 12 size
220 fractions and operated with an air flow of 10 L.min⁻¹. Prior to each measurement, the 13 ELPI
221 impaction stages were cleaned. The corona charger was removed. The electrometer range was
222 set at 400,000 fA, and the baseline was zeroed. The nebulizer was connected to a USP throat
223 via a PTFE mouthpiece adaptor. The USP throat a 90° bend metal pipe with uniform cross
224 section slight contractions at the inlet and a small diffuser at the outlet. Nebulizer aerosolized
225 NaF during 10 minutes, while ELPI V4.0 software recorded current vs. time data for stages 1
226 to 12. Afterwards, the USP throat, corona charger frame, and each stage were rinsed with 5
227 mL of deionized water into appropriate volumetric flasks. Liquids were then assayed for
228 sodium fluoride concentration by electrochemical method indicated by the NF EN 13544-1
229 procedure (perfectION™ combined F⁻ electrode SevenGo pro™, Mettler Toledo, France).
230 The MMAD of nebulized particles was calculated according to the standard NF EN 13544-1
231 using electrochemical measurements of sodium fluoride. The MMAD was interpolated from
232 the particle size distribution curve by noting the particle size at which the line crosses the 50

233 % mark. The geometric standard deviation (GSD) should only be calculated if the particle
234 size distribution curve was reasonably straight between 10 % and 90 %, showing that the
235 aerosol was log-normally distributed. Where a straight line is a good fit to the data, the
236 calculation of GSD was performed by noting the particle size X at which the line crosses the
237 84.13 % mark, and the particle size Y at which the line crosses the 15.87 % mark. Then the
238 Geometric Standard Deviation GSD was calculated from the equation $X/Y^{0.5}$.
239 The NGI allows the collection of nebulized particles from 0.98 μm -14.1 μm into 8 size
240 fractions and operated with an air flow of 15 $\text{L}\cdot\text{min}^{-1}$. The amount of gentamicin impacted at
241 each stage was determined by a residual gravimetric method based on weighing dry filters
242 (Vecellio *et al.*, 2004). The nebulizer was connected to cascade impactor via the nasal plug in
243 order to make the measurements in the same nebulization conditions that performed with the
244 plastinated model. The NGI was cleaned before each experiment. Known weight filters
245 (Gelman, Type A/E, VWR international, France) were placed into the plates of the impactor.
246 The nebulizer equipped with its nasal plug was connected to NGI via the USP. Nasal plug
247 was used in order to make the measurements in the same nebulization conditions that
248 performed with the plastinated model. Solution of gentamicin (4 mL, 80 mg/mL or 4 mL, 40
249 mg/mL) was introduced into the nebulizer and then, vacuum pump and compressor of
250 nebulizer were turned on. Nebulization time was limited to 10 minutes. After, filters were
251 collected and placed at ambient temperature for drying. The USP throat was rinsed with 5 mL
252 of water. Liquid was then placed on a new known weight filter, itself placed with others for
253 drying step. 24h later all filters were again weighted. The amount of gentamicin impacted on
254 filters at each stage in correspondence with each cut-off diameters of the NGI was calculated
255 according to the referred method (Vecellio *et al.*, 2004). Then, MMAD was determined since
256 the cumulative curve mass vs. size according to European standard method NF EN 13544-1.

257

258 *2.6 Drug deposition into the maxillary sinuses*

259 This study assessed the deposition of an active substance on the walls of the maxillary sinuses
260 in a plastinated nasal cast. The main objective was to examine the role of the 100 Hz acoustic
261 frequency on the intrasinus deposition of nebulized drugs. In addition, we wanted to examine
262 the impact of anatomical features (mainly ostium size) and of initial drug concentration
263 introduced into the nebulizer on aerosol deposition. To reach these objectives the gentamicin,
264 an aminoglycoside antibiotic, was used as a marker. We tested both concentrations of
265 gentamicin (*i.e.* 40 mg.mL⁻¹ and 80 mg.mL⁻¹), to determine the impact of the active substance
266 concentration on the aerosol deposition in sinuses. A constant volume of 4 mL of gentamicin
267 solution was nebulized using the NL11SN jet nebulizer. Nebulizations lasted 10 minutes.
268 Experiments were performed either with or without acoustic pressure waves at 100 Hz, and
269 using alternatively a 40 mg.mL⁻¹ or a 80 mg.mL⁻¹ gentamicin solution.

270 After the nebulization, gentamicin was collected from the maxillary sinuses by flushing with
271 physiological serum using a syringe containing 1 mL for the right sinus, and 1 mL for the left
272 sinus (Figure 2). Each sinus was flushed 4 times using the same physiological serum. To
273 avoid overestimation of the amount of gentamicin deposited into the maxillary sinuses, the
274 region close to the maxillary ostium was never flushed. Finally, the gentamicin was quantified
275 in the liquid collected from each maxillary sinus using a fluorescence polarization
276 immunoassay (FPIA) with TDxFLx[®] analyzer (Abbott Diagnostics Division, USA). The
277 detection level of the gentamicin dosage was 0.27 mg.L⁻¹. Each sample was assayed 3 times
278 for each series of measurements and results are expressed as the mean of these 3 values. After
279 recovery, the plastinated nasal cast was washed copiously with tap water during 10 minutes to
280 remove all traces of residual gentamicin. Control nebulizations with physiological saline were
281 randomly performed to verify that the gentamicin content of the flushing liquid collected was
282 lower than the detection level (and therefore to confirm that the plastinated nasal cast washing
283 was efficient). Globally, we have analyzed 286 collected liquid for gentamicin concentration
284 (Table 2).

285 The assay reliability is very important in this work as the main conclusions are based around
286 the deposition of a drug that is quantified. Control nebulizations with physiological saline
287 emphasize the absence in flushing fluid of any extracts from the cast. Thus all traces of
288 residual gentamicin were removed after nebulization experiments. Besides, the impact of
289 matrix effects on overall analytical performance and the potential usability of the data were
290 determined using a spiked matrix sample. Hence, we used a representative environmental
291 sample that has known concentration of gentamicin prior to being taken through the entire
292 analytical process in order to evaluate bias. 1 mL of solution at 2.35 mg.L⁻¹ of gentamicin was
293 introduced into the maxillary sinuses to simulate an intrasinus drug deposition after
294 nebulization. The drug recovery efficiency of the methodology used was always in the 85-
295 93% range (*i.e* we measure a gentamicin concentration between 2 and 2.15 mg.L⁻¹ in the
296 flushing fluid). These results confirm a good accuracy of the methodology of drug deposition
297 quantification into the maxillary sinuses.

298

299 *2.7 Statistical analysis*

300 Metrologic data obtained from cascade impactors (MMAD) and from output measurements
301 were analyzed using non-parametric tests. Theses statistical test are adapted to small samples
302 size and were performed with StatXact[®] software (Cytel, France). Significance was
303 established with permutation test (p<0.05).

304 The influence of using sonic mode during nebulization and the influence of gentamicin
305 concentration on the gentamicin deposition into maxillary sinuses, data obtained from
306 experiments performed with the plastinated head model were analyzed with t-test (on
307 XLSTAT[®] software, Addinsoft, USA). A p<0.05 was considered significantly.

308

309 **3. Results**

310 *3.1 Anatomical features of the plastinated human nasal cast*

311 The clinical anatomy study by nasofiberoscopy showed that the plastinated nasal specimen
312 was very similar to living anatomical conditions observed daily by ENT physicians. All
313 anatomical details were well-preserved. CT scans confirmed the high preservation of the nasal
314 airway anatomy as well as that of the mucosa of the turbinates (Figure 3). Interestingly, the
315 plastinated specimen exhibited very dissimilar maxillary ostium morphologies. Indeed, while
316 the right maxillary sinus ostium appeared as anatomically usual, the left maxillary ostium was
317 doubtless abnormally short and broad. In particular, the diameter of the left maxillary sinus
318 ostium was three times higher than that of the right maxillary sinus ostium. However, the
319 acoustic rhinometry reasonably resolved the airways geometry of the plastinated cast. We
320 found a perfect symmetry between the left and right nasal cavities with a minimal cross-
321 sectional area around 0.5 cm^2 and a cross-sectional area higher than 1.5 cm^2 from the middle
322 meatus region (Figure 4) (Durand et al., 2011).

323

324 *3.2 Aerodynamic behaviour of the plastinated human nasal cast*

325 We also measured by rhinomanometry the resistance of each nasal cavity separately while the
326 opposite nostril was occluded. From the pressure vs. flow curves, the unilateral airflow
327 resistances found, for left and right nasal cavities, were perfectly similar at $0.18 \text{ Pa.s.cm}^{-3}$ (*i.e.*
328 $1.8 \text{ cmH}_2\text{O.s.L}^{-1}$). The bilateral airflow resistance was, logically, lower than unilateral
329 resistances, around $0.13 \text{ Pa.s.cm}^{-3}$. Finally, very original data were obtained by examining the
330 airflow serial resistance of both the maxillary ostium and the nasal cavity. Results emphasized
331 very disparate airflow resistances: $0.73 \text{ Pa.s.cm}^{-3}$ for the left nasal cavity in serial with the left
332 maxillary ostium, and $1.21 \text{ Pa.s.cm}^{-3}$ for the right nasal cavity in serial with the right
333 maxillary ostium. Because the uninasal airflow resistances of the left and right nasal cavities
334 are rigorously identical ($0.18 \text{ Pa.s.cm}^{-3}$), this result suggests that morphology changes of the
335 maxillary ostium could have a huge impact on sinus ventilation. Indeed, the low airflow
336 resistance put in evidence for the left nasal cavity in serial with the left maxillary ostium is in

337 good agreement with the abnormally short and broad ostium of the left maxillary sinus as
338 determined from CT scans (Figure 3) (Durand et al., 2011).

339

340 *3.3 Signal processing of the acoustic airflow*

341 The maximum acoustic pressure level generated at 100 Hz from the NL11SN was equal to
342 107 dB at 1 cm of the output pipe. The distance of measurement has been empirically chosen
343 but it allowed relative measurements. Theoretically the signal must be a 100 Hz sinusoidal
344 signal, but our results highlight that it is not exactly sinusoidal, as shown in Figure 5A. Then,
345 a spectral analysis using the Fourier transform was performed in order to have a better
346 understanding of the frequency components of the signal (Figure 5B). The main component of
347 the signal is 100 Hz as expected, but there are three other harmonic components at 200, 300
348 and 400 Hz respectively. The fundamental amplitude is about ten times higher than the
349 harmonics amplitudes. The harmonics are certainly due to the resonance of the pipe which
350 behaves like a wind instrument.

351

352 *3.4 Aerosol metrology*

353 ELPI results using NaF as a marker emphasize a significant decrease of MMAD in presence
354 of the 100 Hz acoustic airflow of about 35 % ($3.45 \pm 0.25 \mu\text{m}$ vs $5.40 \pm 0.15 \mu\text{m}$). NGI results
355 using gentamicin as a marker indicate that MMAD significantly increased when the
356 gentamicin concentration rises (Figure 6). In accordance with ELPI measurements, NGI
357 results show also that adding the 100 Hz acoustic frequency during nebulization led to
358 decrease the MMAD for a given gentamicin concentration (Figure 6).

359 The aerosol output measurements emphasize a huge impact of 100 Hz acoustic frequency. A
360 significant decrease, about 60%, of the amount of gentamicin aerosolized in presence of 100
361 Hz acoustic frequency was highlighted (Table 2). Without acoustic pressure waves 17-20 %

362 of the volume of gentamicin initially introduced was nebulized, although only 7-8 % was
363 nebulized in presence of 100 Hz acoustic airflow.

364

365 *3.5 Drug deposition into the maxillary sinuses*

366 We sequentially studied the influence of three parameters: the 100 Hz acoustic airflow, the
367 gentamicin concentration, and the maxillary ostium anatomical features. Results obtained
368 clearly show that:

369 ➤ At 80 mg.mL⁻¹, the drug deposition is higher in the left maxillary sinus cavity than in the
370 right one, either in presence or in absence of acoustic airflow (Figure 7 – Table 3). As a result
371 the endonasal anatomical features seem to play a major role on aerosol deposition.

372 ➤ Whatever the initial gentamicin concentration used, the drug deposition in left and right
373 sinus cavities is higher in presence of 100 Hz acoustic frequency than without acoustic
374 airflow. We emphasized that the 100 Hz acoustic airflow led to increase at least 2 fold the
375 drug deposition in the maxillary sinuses for a given maxillary ostium anatomical feature
376 (Figure 7 – Table 3).

377 ➤ Both in presence and in absence of acoustic airflow, an increased gentamicin concentration
378 induced an increased drug deposition in the right as well as in the left maxillary sinuses
379 (Figure 7 – Table 3).

380

381 **4. Discussion**

382 *4.1 Influence of 100 Hz acoustic airflow on intrasinus drug deposition*

383 Measurements made using the plastinated nasal cast doubtless highlight that the addition of a
384 100 Hz acoustic airflow to the gentamicin aerosol leads to a 2 to 3 fold increase drug
385 deposition into the maxillary sinuses depending on nebulization conditions (Figure 7).
386 Moreover, it is interesting to examine the gain of drug deposition by the 100 Hz acoustic
387 airflow comparing the results with and without a 100 Hz acoustic frequency, all other factors

388 being exactly the same (*i.e.* on the same sinus and gentamicin concentration). The gain in
389 drug deposition brought about by the addition of a 100 Hz acoustic frequency to the aerosol
390 production is identical, whatever the anatomic and aerodynamic endonasal features, and in
391 particular, whatever the characteristics of the maxillary ostium (Figure 8). However, this drug
392 deposition gain is even more important when the initial concentration of gentamicin decreases
393 (deposition gain of about 100 % at 80 mg.mL⁻¹ vs. a deposition gain of about 220 % at 40
394 mg.mL⁻¹). As a result, the gain of sinus drug deposition brought by the 100 Hz acoustic
395 frequency strongly depends on the gentamicin concentration initially introduced into the
396 nebulizer.

397 The metrology study indicated that the 100 Hz acoustic frequency significantly reduced the
398 MMAD of the particles produced by the NL11SN and the aerosol output (Figure 6, Table 2).
399 The decrease of MMAD varies from 10 % to 27 % depending on the initial gentamicin
400 concentration. In the same time, the decrease of aerosol output is about 60 % whatever the
401 initial gentamicin concentration. Doubtless, the amount of gentamicin inhaled, for a same
402 nebulization time, is less important in presence of acoustic airflow since the MMAD and the
403 aerosol output decrease. However, as the gentamicin concentration collected into maxillary
404 sinus is greater when nebulization is performed with a 100 Hz acoustic frequency, we suggest
405 that the amount of particles penetrating into the maxillary sinus is more important in presence
406 of a 100 Hz acoustic frequency.

407 Overall, the mechanism underlying the augmentation of drug deposition in presence of 100
408 Hz acoustic frequency was probably due to a balance between a decrease of particle size and
409 aerosol output, and an increase of the number of the airborne particles reaching the maxillary
410 sinuses.

411 But a key question remains: why does the number of airborne particles reaching the maxillary
412 sinuses rise in presence of 100 Hz acoustic frequency? A first explanation could be the
413 smaller particle size induced by the acoustic pressure waves, despite the simultaneous

414 decrease of the aerosol output. But in fact, for specific experimental conditions, the rise of
415 gentamicin concentration can balance the influence of the 100 Hz acoustic frequency on
416 particle size and on aerosol output. As an example, the MMAD of particles produced by the
417 NL11SN is almost the same when the 40 mg.mL⁻¹ gentamicin solution is nebulized without
418 100 Hz acoustic frequency or when the 80 mg.mL⁻¹ gentamicin solution is nebulized with an
419 acoustic airflow (2.21 ± 0.14 μm and 2.54 ± 0.04 μm respectively). Therefore, if the transport
420 mechanism for a same particle size was similar in presence or in absence of 100 Hz acoustic
421 frequency, the amount of gentamicin deposited into the maxillary sinuses when nebulized at
422 40 mg.mL⁻¹ without a 100 Hz acoustic frequency should be expected to be 1.5-fold higher
423 (because of the gentamicin concentration is twice while the aerosol output is about 3 times
424 lower) than the amount deposited during sonic nebulization of 80 mg.mL⁻¹ of gentamicin.
425 However, the drug deposition rose by a factor 6 to 8. Consequently, for the same particle size,
426 the presence of acoustic frequency increases by approximately a factor 5 the number of
427 particles deposited into the maxillary sinuses independently of the acoustic frequency effect
428 on particle size and aerosol output.

429 Thus, our results strongly support the existence of a specific transport mechanism of
430 particles through ostium in the presence of 100 Hz acoustic frequency. Recently, Maniscalco
431 *et al.* showed that an oscillating airflow produced by phonation (nasal humming) caused a
432 large increase in the gas exchange between the nose and the paranasal sinuses (Maniscalco *et*
433 *al.*, 2006). Moreover, these authors also demonstrated that the gas ventilation between the
434 nose and sinuses was even more important when the frequency of the acoustic airflow used
435 was closed to the resonant frequency of the sinus cavity (Maniscalco *et al.*, 2006-2). In fact, a
436 cavity of air with an opening will resonate at a natural frequency when the air is excited, as
437 the well-known principle of the Helmholtz resonator (Kinsler *et al.*, 1962). Indeed, when air is
438 forced into a cavity, the pressure inside increases. When the external force pushing the air into
439 the cavity is removed, the higher-pressure air inside will flow out. However, this surge of air

440 flowing out will tend to over-compensate, due to the inertia of the air in the neck, and the
441 cavity will be left at a pressure slightly lower than outside, causing air to be drawn back in.
442 This process repeats with the magnitude of the pressure changes decreasing each time. All
443 things considered, we support the conclusion that the sinus cavity could be compared in a first
444 approximation to a Helmholtz resonator. In this sense, the maxillary sinus can be comparable
445 to a resonator system that exhibits resonant behaviour in presence of 100 Hz acoustic
446 frequency. This assumption is in perfect accordance with previous work which estimated the
447 fundamental resonant frequencies of paranasal sinuses in the range 110-350 Hz using the
448 Helmholtz resonator theory (Tarhan *et al.*, 2005).

449

450 *4.2 Impact of maxillary ostium anatomical and aerodynamical characteristics on drug* 451 *deposition*

452 We demonstrated that the aerosols can penetrate into the maxillary sinuses even if we
453 observed a differential deposition of active substance as a function of maxillary ostium
454 anatomical features. As a matter of fact the amount of nebulized active substance collected
455 into the sinus is higher in the left sinus of our plastinated nasal cast. This left sinus was
456 characterized by a short and broad maxillary ostium inducing a weak airflow resistance to
457 sinus ventilation. As a result the endonasal anatomic conditions (and the airflow resistance
458 associated) have certainly a huge impact on drug deposition into maxillary sinuses.

459 Nevertheless, we also emphasized a significant drug deposition for long and quite narrow
460 maxillary ostium (right nasal cavity of the plastinated nasal cast). The fact that a small size of
461 the ostium allows an effective drug deposition is quite encouraging to extrapolate results to
462 diseased subject. It is obvious that nasal airway obstruction in patients with rhinosinusitis as
463 well as complete closure of the maxillary ostia prevent any drug deposition into the sinuses.
464 However, we have the demonstration that aerosols can penetrate into the maxillary sinuses in
465 the case of quite unfavorable anatomic and aerodynamic endonasal conditions. This result

466 seems to be a major value of proving that nebulized drug can reach the middle meatus, which
467 is considered to be the most common area for sinusitis disorders. In this sense our results
468 show that the use of 100 Hz acoustic frequency during nebulization may provide sufficient
469 drug delivery for a topical aerosol therapy in sinonasal disorders. Nevertheless clinical trials
470 are required to definitively conclude on the clinically efficiency because of the nasal cast
471 differed from *in vivo* mainly due to the absence of mucus or breathing with the plastinated
472 cast.

473

474 **5. Conclusion**

475 The plastinated nasal cast appeared useful for *in vitro* characterization of drug deposition into
476 maxillary sinuses. We demonstrated that antibiotic aerosol can penetrate into the maxillary
477 sinuses. We also emphasized a great efficiency of the 100 Hz acoustic airflow to enhance
478 drug deposition into maxillary sinuses. A significant increase (2 to 3-fold) of intrasinus drug
479 deposition was obtained in presence of 100 Hz acoustic frequency, despite the decrease of
480 60% of the aerosol output induced by the acoustic pressure waves. Thus, the acoustic effect
481 allows the improvement of targeting of nebulized antibiotics to the maxillary sinuses, and
482 even with the lower concentration of antibiotics nebulized (a great advantage to limit side-
483 effect and to prevent potential antibiotic resistance). We also established that the addition of
484 the 100 Hz acoustic frequency reduces the aerodynamic particle size (MMAD). Moreover, the
485 gain of drug deposition observed in presence of acoustic airflow was independent of the
486 anatomical and aerodynamical characteristics of the maxillary ostium. These results suggest
487 that a specific transport mechanism of airborne particle occurs during an acoustic airflow
488 nebulization. The mechanisms seem to induce a significant rise of the number of particles
489 penetrating into the maxillary sinus independently of changes on particle size and aerosol
490 output. The comparison of the sinus cavity to a Helmholtz resonator could, at least partially,
491 explain the phenomenon observed. Finally, we demonstrated that the gain of drug deposition

492 observed with 100 Hz acoustic frequency depends on the gentamicin concentration initially
493 introduced into the nebulizer. Therefore, this result indicates that specific drug and/or specific
494 dosages should be selected to fully benefit from the deposition enhancement brought by the
495 100 Hz acoustic airflow nebulizer.

496

497 **Conflict of interest**

498 S. Le Guellec is an employee of Diffusion Technique Française (DTF Medical, Saint Etienne,
499 France).

500

501 **References**

502 Cakmak, O., Celik, H., Cankurtaran, M., Buyuklu, F., Ozgirgin, N., Ozluoglu, L.N.,
503 2003. Effects of paranasal sinus ostia and volume on acoustic rhinometry measurements: a
504 model study. *J Appl Physiol.* 94:1527-1535

505 Croce, C., Fodil, R., Durand, M., Sbirlea-apiou, G., Caillibotte, G., Papon, J.F.,
506 Blondeau, J.R., Coste, A., Isabey, D., Louis, B., 2006. In vitro experiments and numerical
507 simulations of airflow in realistic nasal airway geometry. *Ann Biomed Eng.* 34:997-1007.

508 Durand, M., Pourchez, J., Louis, B., Pouget, J.F., Isabey, D., Coste, A., Prades, J.M.,
509 Rusch, P., Cottier, M., 2011. Plastinated nasal model: a new concept of anatomically realistic
510 cast. *Rhinology.* 49(1), 30-36.

511 Durand, M., Rusch, P., Granjon, D., Chantrel, G., Prades, J.M., Dubois, F., Esteve, D.,
512 Pouget, J.F., Martin, C., 2001. Preliminary study of the deposition of aerosol in the maxillary
513 sinuses using a plastinated model. *J Aerosol Med.* 14:83-93.

514 Fokkens, W.J., Lund, V.J., Mullol, J. *et al.*, 2007. European Position Paper on
515 Rhinosinusitis and Nasal Polyps. *Rhinology.* 45; suppl. 20: 1-139.

516 Guillerm, R., Badre, R., Flottes, L., Riu R., Rey, A., 1959. A new method of aerosol
517 penetration into the sinuses (in french). *Presse Med.* 67:1097-1098.

518 Kinsler, L.E., Frey, A.R., 1962. Fundamentals of acoustics (2nd ed.). New York: Wiley.

519 Hilton, C., Wiedmann, T., St. Martin, M., Humphrey, B., Schleiffarth, R., Rimell, F.,
520 2008. Differential deposition of aerosols in the maxillary sinus of human cadavers by particle
521 size. *Am J Rinol.* 22:395-398.

522 Hyo, N., Takano, H., Hyo, Y., 1989. Particle deposition efficiency of therapeutic
523 aerosols in the human maxillary sinus. *Rhinology.* 27:17-26.

524 Maniscalco, M., Sofia, M., Weitzberg, E., Lundberg, J.O., 2006. Sounding airflow
525 enhances aerosol delivery into the paranasal sinuses. *Eur J Clin Invest.* 36(7):509-513.

526 Maniscalco, M., 2006-2. Humming nitric oxide and paranasal sinus ventilation. In:
527 Thesis. Karolinska University Press, Stockholm, Sweden.

528 Marple, V.A.; Olson, B.A.; Santhanakrishnan, K.; Roberts, D.L.; Mitchell, J.P.;
529 Hudson-Curtis, B.L., 2004. Next generation pharmaceutical impactor: a new impactor for
530 pharmaceutical inhaler testing. Part III. extension of archival calibration to 15 L/min. *J*
531 *Aerosol Med.*;17(4):335-43.

532 Moeller, W., Schuschnig, U., Meyer, G., Mentzel, H., Keller, M., 2008. Ventilation and
533 drug delivery to the paranasal sinuses: studies in a nasal cast using pulsating airflow.
534 *Rhinology.* 46:213-220.

535 Moeller, W., Schuschnig, U., Saba, G.K., Meyer, G., Junge-Hulsing, B., Keller, M.,
536 Haussinger, K., 2010. Pulsating aerosols for drug delivery to the sinuses in healthy volunteers.
537 *Otolaryngol Head Neck Surg.* 142:382-388.

538 Saijo, R., Majima, Y., Hyo, N., Takano, H., 2004. Particle deposition efficiency of
539 therapeutic aerosols in the nose and paranasal sinuses after transnasal sinus surgery. *Am J*
540 *Rinol.* 18:1-7.

541 Schreck, S., Sullivan, K.J., Ho, C.M., Chang, H.K., 1993. Correlation between flow
542 resistance and geometry in a model of the human nose. *J Appl Physiol.* 75:1767-1775.

543 Kelly, J.T., Prasad, A.K., Wexler, A.S., 2000. Detailed flow patterns in the nasal cavity.
544 J. Appl. Physiol. 51:5-19.

545 Tarhan, E., Coskun, M., Cakman, O., Celik, H., Cankurtaran, M., 2005. Acoustic
546 rhinometry in humans: accuracy of nasal passage area estimates, and ability to quantify
547 paranasal sinus volume and ostium size. J. Appl Physiol. 99:616-623.

548 Vaughan, W.C., Carvalho, G., 2002. Use of nebulized antibiotics for acute infections in
549 chronic sinusitis. Otolaryngol Head Neck Surg. 126:558-568.

550 Vecellio, L., De Gersem, R., Le Guellec, S., Reychler, G., Pitance, L., . Le Penneec, D.,
551 Diot, P., Chantrel, G., Bonfils, P., Jamar, F., 2011. Deposition of aerosols delivered by nasal
552 route with jet and mesh nebulizers, International Journal of Pharmaceutics. 407:87-94.

553 Vecellio, L., Grimbert, D., Bordenave, J., Benoit, G., Furet, Y., Fauroux, D., Boissinot,
554 E., de Monte, M., Lemarie, E., Diot, P., 2004. Residual gravimetric method to measure
555 nebulizer output. J Aerosol Med Deposit Clearance Effects Lung. 17:63-71.

556 von Hagens, G., 1979. Impregnation of soft biological specimens with thermosetting
557 resins and elastomer. Anat. Rec. 194:247-255.

558

Impact of Acoustic Airflow Nebulization on Intranasal Drug Deposition of a Human Platinated Nasal Cast: New Insights into the Mechanisms involved

Marc DURAND ^{1,2,3}, Jérémie POURCHEZ ^{2,3,4*}, Gérald AUBERT ⁵, Sandrine LE GUELLEC ^{6,7}, Laurent NAVARRO ^{3,4}, Valérie FOREST ^{2,3,4}, Philippe RUSCH ^{2,3,5,8,9}, Michèle COTTIER ^{2,3,5,8,9}

¹ Centre Hospitalier Emile Roux, F-43012, Le Puy en Velay, France

² LINA, Laboratoire Interdisciplinaire d'étude des Nanoparticules Aérosolisées, EA 4624, F-42023, Saint-Etienne, France

³ SFR IFRESIS, F-42023, Saint-Etienne, France

⁴ Ecole Nationale Supérieure des Mines de Saint-Etienne, Centre Ingénierie et Santé, F-42023, Saint-Etienne, France

⁵ CHU de Saint-Etienne, F-42055, Saint-Etienne, France

⁶ DTF-Aerodrug, Faculté de médecine, F-37032, Tours, France

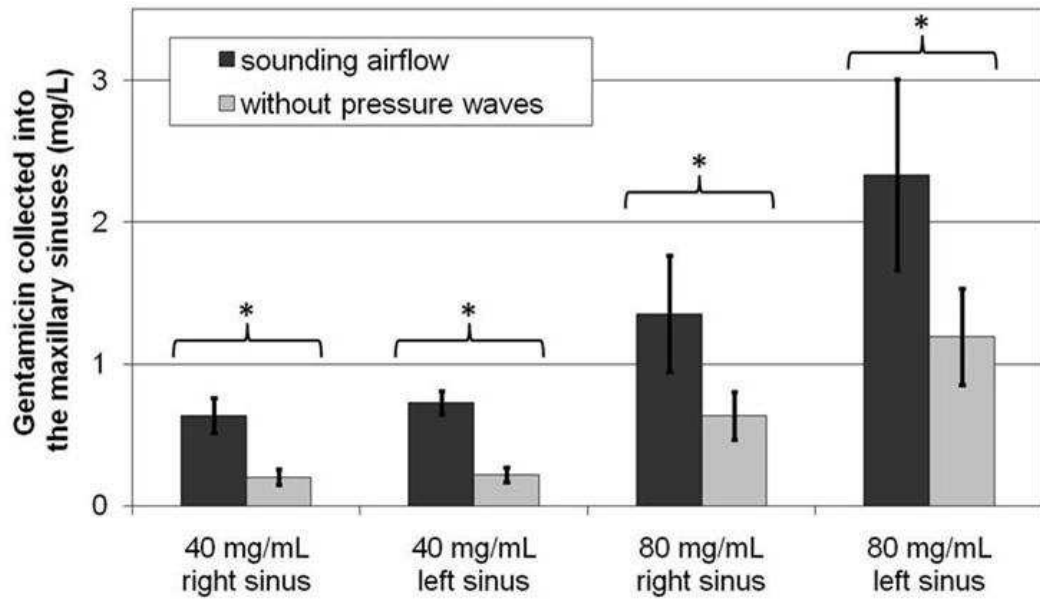
⁷ INSERM-U618, Faculté de Médecine, F-37032, Tours, France

⁸ Université Jean Monnet, Faculté de Médecine, F-42023, Saint-Etienne, France

⁹ Université de Lyon, F-42023, Saint-Etienne, France

* Corresponding author: Tel: (+33) 4 77 42 01 80; Fax: (+33) 4 77 49 96 94;
E-mail address: pourchez@emse.fr

Graphical abstract



Impact of Acoustic Airflow Nebulization on Intranasal Drug Deposition of a Human Plastinated Nasal Cast: New Insights into the Mechanisms involved

Marc DURAND^{1,2,3}, Jérémie POURCHEZ^{2,3,4*}, Gérald AUBERT⁵, Sandrine LE GUELLEC^{6,7}, Laurent NAVARRO^{3,4}, Valérie FOREST^{2,3,4}, Philippe RUSCH^{2,3,5,8,9}, Michèle COTTIER^{2,3,5,8,9}

¹ Centre Hospitalier Emile Roux, F-43012, Le Puy en Velay, France

² LINA, Laboratoire Interdisciplinaire d'étude des Nanoparticules Aérosolisées, EA 4624, F-42023, Saint-Etienne, France

³ SFR IFRESIS, F-42023, Saint-Etienne, France

⁴ Ecole Nationale Supérieure des Mines de Saint-Etienne, Centre Ingénierie et Santé, F-42023, Saint-Etienne, France

⁵ CHU de Saint-Etienne, F-42055, Saint-Etienne, France

⁶ DTF-Aerodrug, Faculté de médecine, F-37032, Tours, France

⁷ INSERM-U618, Faculté de Médecine, F-37032, Tours, France

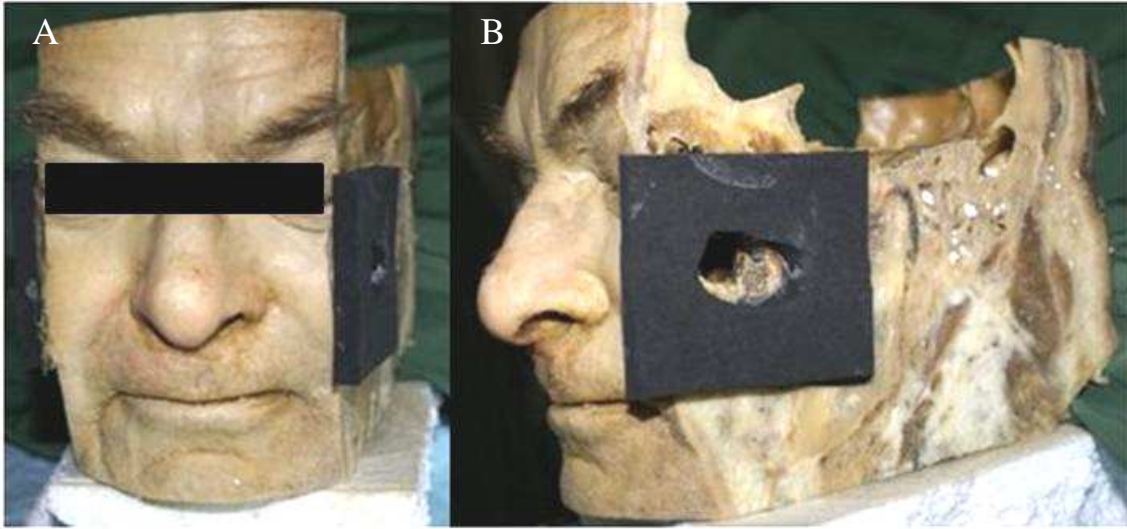
⁸ Université Jean Monnet, Faculté de Médecine, F-42023, Saint-Etienne, France

⁹ Université de Lyon, F-42023, Saint-Etienne, France

* Corresponding author: Tel: (+33) 4 77 42 01 80; Fax: (+33) 4 77 49 96 94;
E-mail address: pourchez@emse.fr

1

Figure 1



2

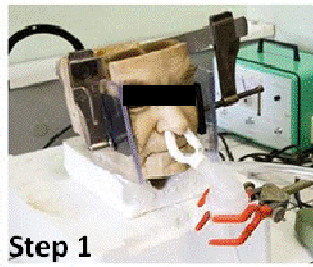
3

4 Figure 1: Plastinated head model elaborated by a specific plastination procedure and used as a
5 nasal cast to assess the deposition of drug into the maxillary sinuses. (A) represents the
6 anterior view and (B) represents the lateral view showing the exterior free access to the left
7 maxillary sinuses.

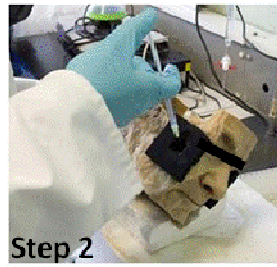
8

9
10

Figure 2



Step 1
Nebulization of gentamicin solution during 10 minutes



Step 2
Collection of Gentamicin from the maxillary sinuses by flushing the cavity with physiological serum



Quantification of the gentamicin collected thanks to a fluorescence polarization immunoassay

Step 3

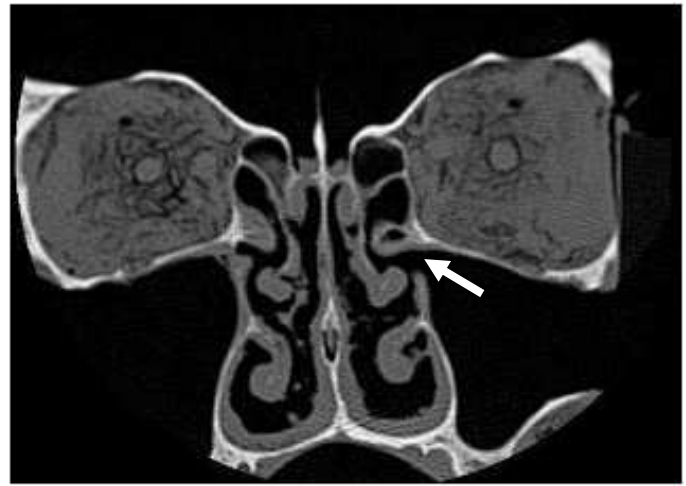
11
12

13
14
15
16
17

Figure 2: Overall description of the drug deposition assessment procedure on the plastinated nasal cast.

18

Figure 3



19

20

21

22

Figure 3: CT scans performed on the plastinated specimen. Observation of the high

23

preservation of the mucosa and of the different morphology of the maxillary ostia on both

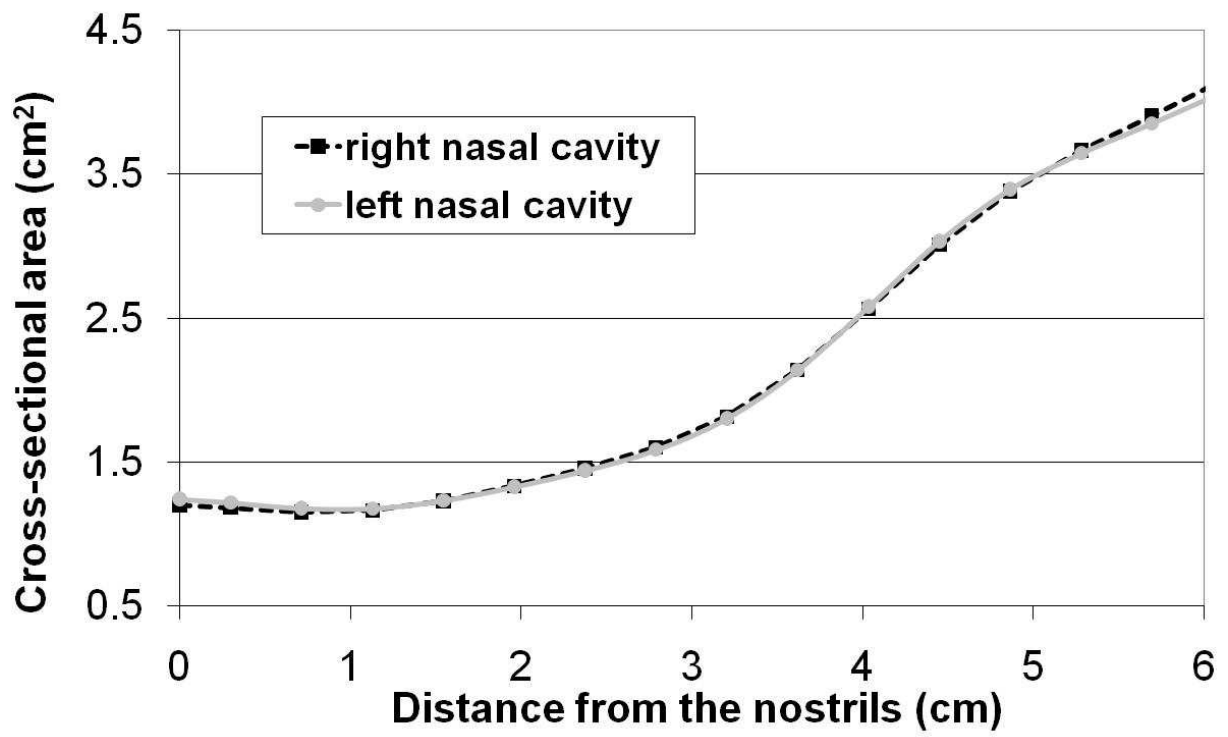
24

side (white arrows indicate maxillary ostia).

25

26

Figure 4



27

28

29

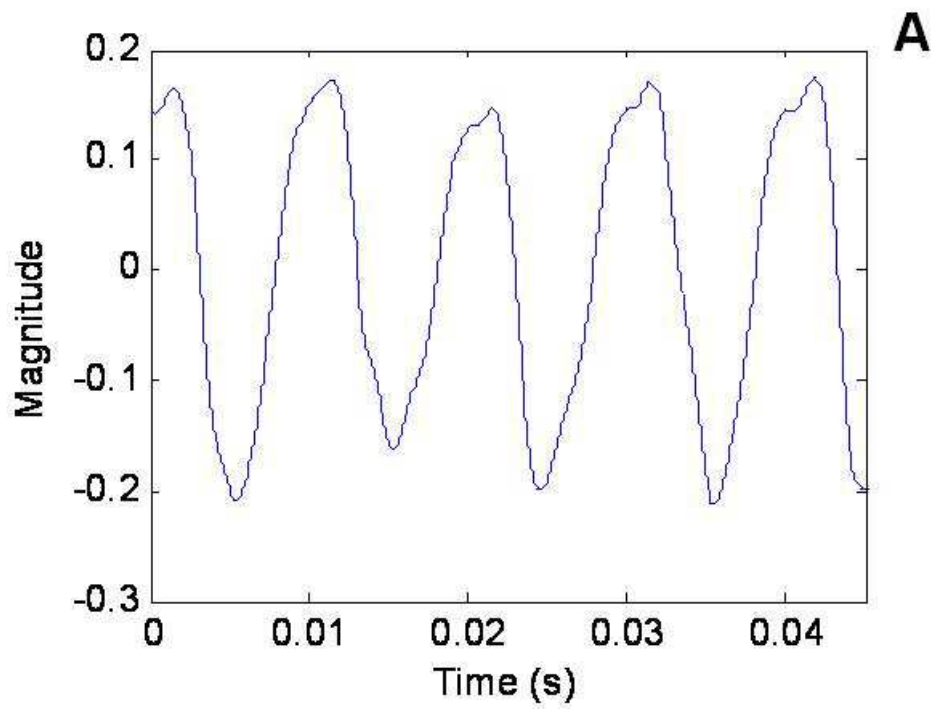
30

Figure 4: Acoustic rhinometry results obtained on the plastinated nasal cast.

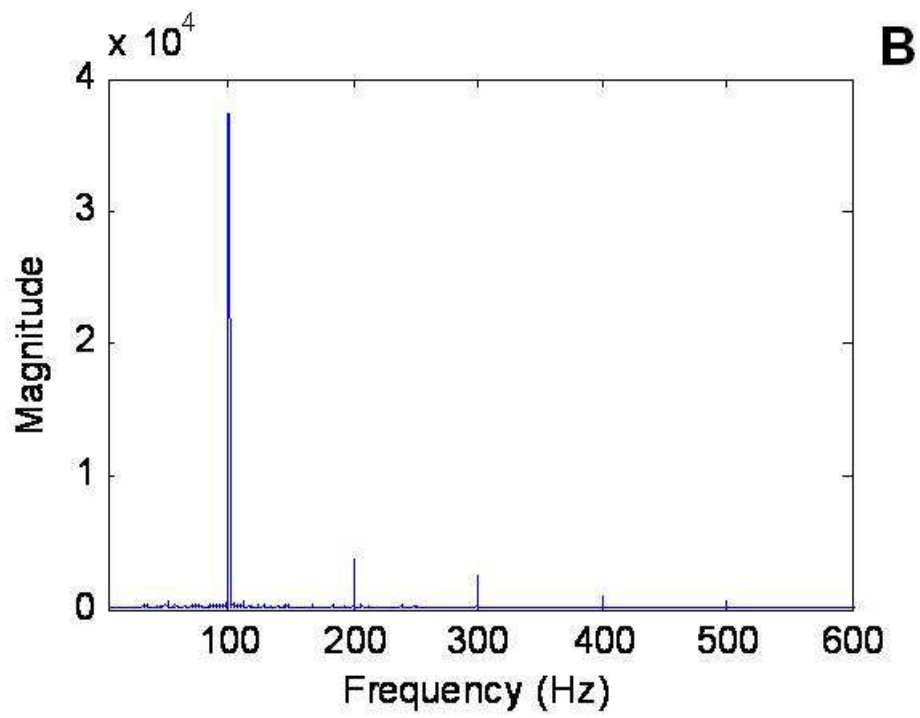
31

32

Figure 5



33



34

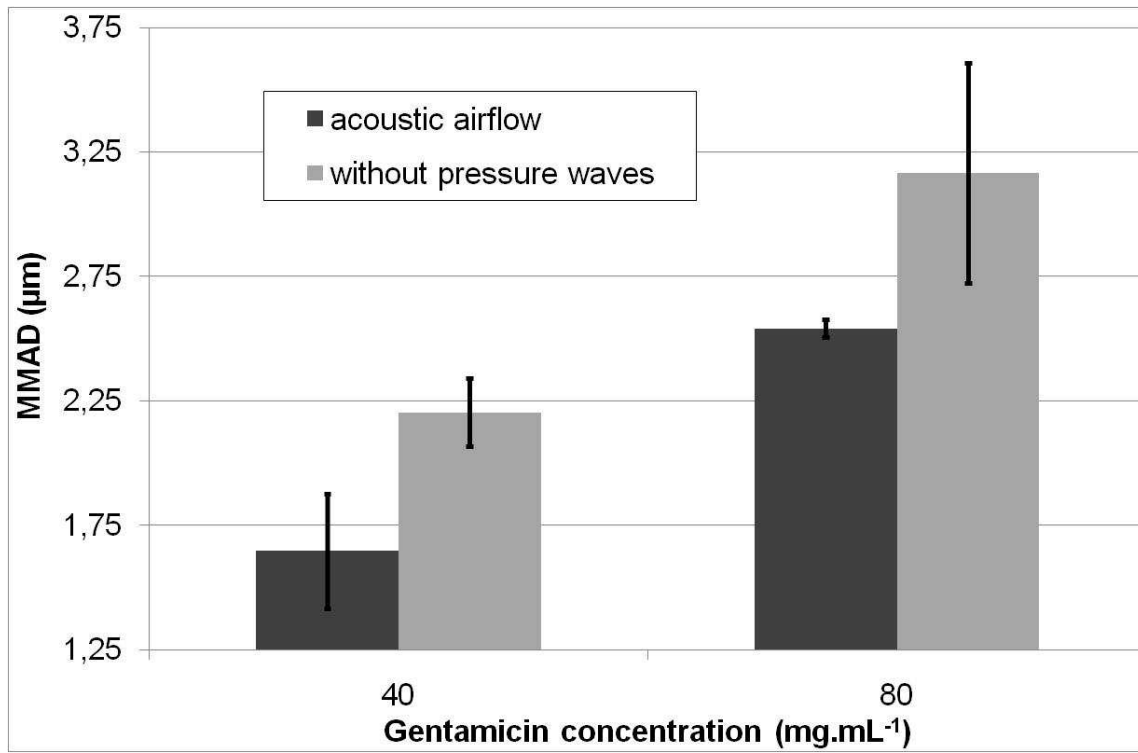
35

36
37
38
39
40
41

Figure 5: Signal processing of the 100 Hz sound added to the aerosol during its production by the NL11SN nebulizer / AOLH[®] compressor / AS[®] sonic generator: shape of the acoustic signal (A) and spectral analysis using the Fourier transform (B).

42
43

Figure 6



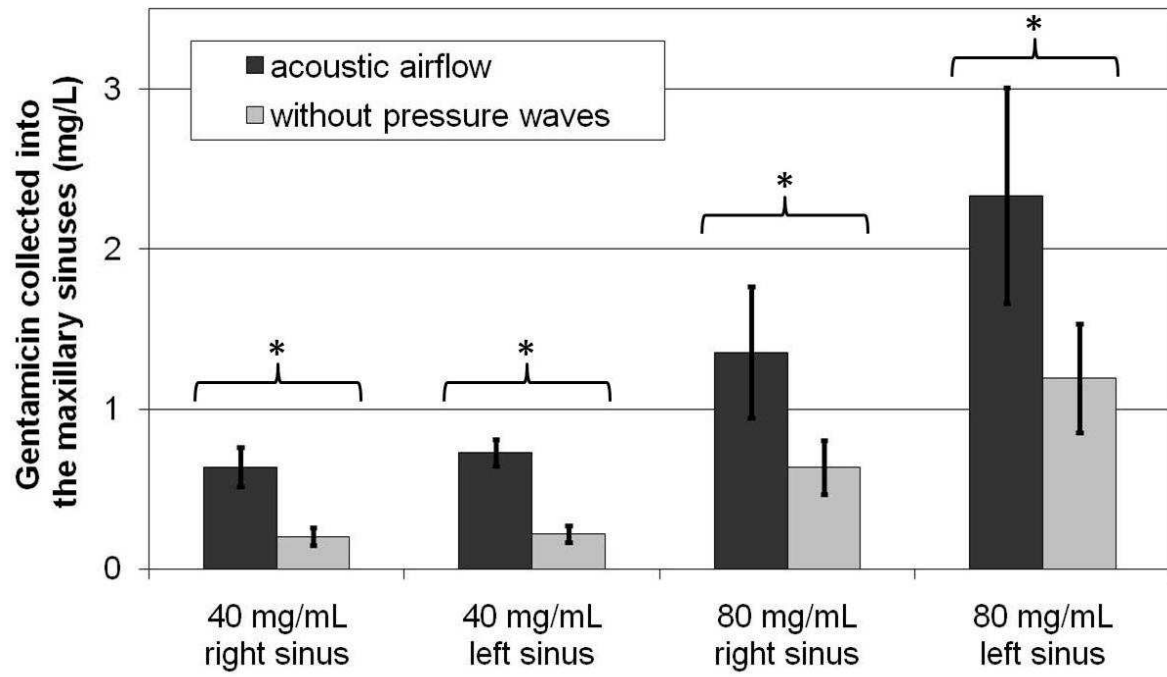
44

45
46
47
48
49
50

Figure 6: Impact of nebulization conditions (100 Hz acoustic airflow and gentamicin concentration) on the metrology of airborne particle measured using the NGI impactor (Permutation test: MMAD without sound pressure waves *vs.* MMAD with acoustic airflow: $p = 0.0007$; MMAD at 40 mg.mL^{-1} *vs.* MMAD at 80 mg.mL^{-1} : $p = 0.005$).

51
52

Figure 7



53

54

55

Figure 7: Influence of a 100 Hz acoustic airflow on the amount of nebulized gentamicin

56

collected into the maxillary sinuses of the plastinated nasal cast (* : comparisons are

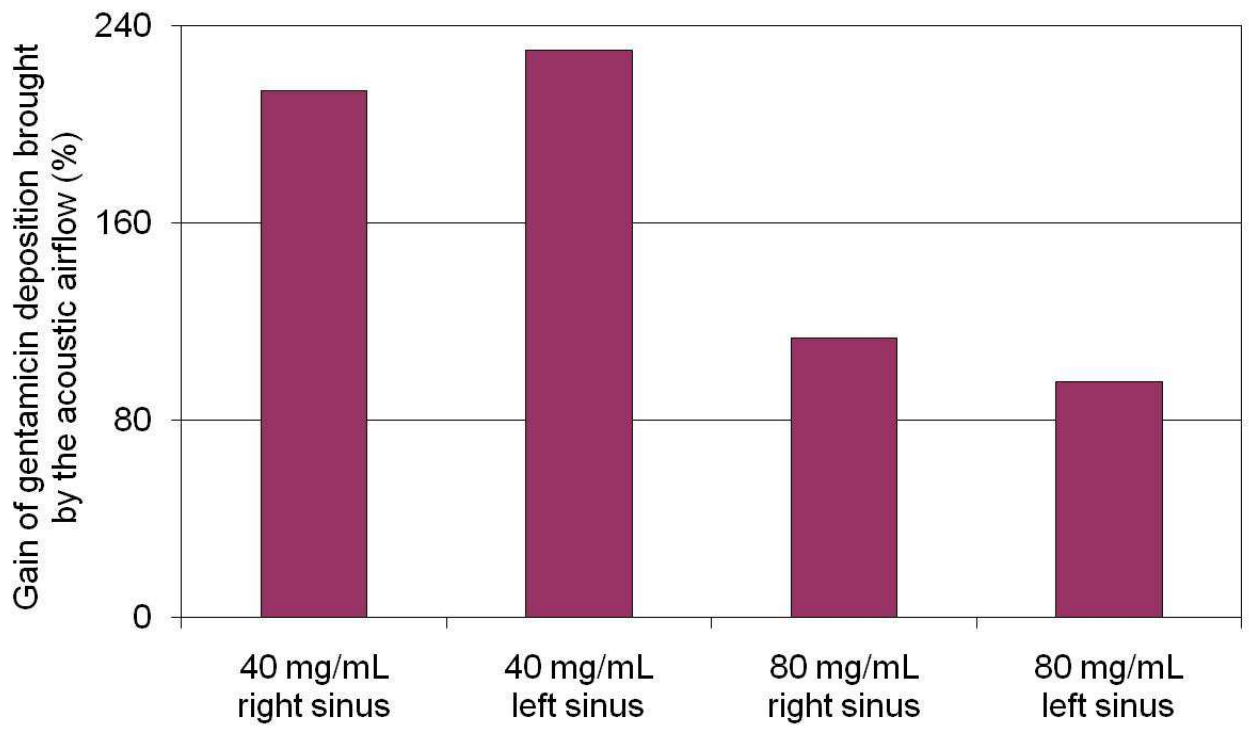
57

statistically significant).

58

59

Figure 8



62
63
64
65
66
67
68
69
70
71
72

Figure 8: Influence of the endonasal anatomical features and the initial gentamicin concentration introduced into the nebulizer on the sinus deposition gain brought by the 100 Hz acoustic airflow (in comparison with experiments without sound pressure waves).

Impact of Acoustic Airflow Nebulization on Intranasal Drug Deposition of a Human Plastinated Nasal Cast: New Insights into the Mechanisms involved

Marc DURAND^{1,2,3}, Jérémie POURCHEZ^{2,3,4*}, Gérald AUBERT⁵, Sandrine LE GUELLEC^{6,7}, Laurent NAVARRO^{3,4}, Valérie FOREST^{2,3,4}, Philippe RUSCH^{2,3,5,8,9}, Michèle COTTIER^{2,3,5,8,9}

¹ Centre Hospitalier Emile Roux, F-43012, Le Puy en Velay, France

² LINA, Laboratoire Interdisciplinaire d'étude des Nanoparticules Aérosolisées, EA 4624, F-42023, Saint-Etienne, France

³ SFR IFRESIS, F-42023, Saint-Etienne, France

⁴ Ecole Nationale Supérieure des Mines de Saint-Etienne, Centre Ingénierie et Santé, F-42023, Saint-Etienne, France

⁵ CHU de Saint-Etienne, F-42055, Saint-Etienne, France

⁶ DTF-Aerodrug, Faculté de médecine, F-37032, Tours, France

⁷ INSERM-U618, Faculté de Médecine, F-37032, Tours, France

⁸ Université Jean Monnet, Faculté de Médecine, F-42023, Saint-Etienne, France

⁹ Université de Lyon, F-42023, Saint-Etienne, France

* Corresponding author: Tel: (+33) 4 77 42 01 80; Fax: (+33) 4 77 49 96 94;
E-mail address: pourchez@emse.fr

1

Table 1

Nebulization conditions			Metrology experiments		
<i>Type of marker</i>	<i>Volume and concentration</i>	<i>With (w) or without (wo) acoustic airflow</i>	<i>ELPI</i>	<i>NGI</i>	<i>Output</i>
NaF	4 mL 2.5% wt	w	n=3		
NaF	4 mL 2.5% wt	wo	n=3		
Gentamicin	4 mL 40 mg.mL ⁻¹	w		n = 3	n=3
Gentamicin	4 mL 40 mg.mL ⁻¹	wo		n = 3	n=3
Gentamicin	4 mL 80 mg.mL ⁻¹	w		n = 3	n=3
Gentamicin	4 mL 80 mg.mL ⁻¹	wo		n = 3	n=3

2

3

4

5

Table 1: Design of the metrology experiments conducted during the study.

6

7
8

Table 2

Nebulization conditions	Type of nebulization	Number of experiments (gentamicin dosage)	Aerosol output results
Control nebulization with physiological saline solution (4 mL without gentamicin)	10 minutes nebulization	66	-
Gentamicin solution (4 mL at 40 mg.mL ⁻¹)	10 minutes nebulization “classic” operating mode	62	0.83 ± 0.05 mL
Gentamicin solution (4 mL at 40 mg.mL ⁻¹)	10 minutes nebulization “sonic” operating mode	54	0.32 ± 0.02 mL
Gentamicin solution (4 mL at 80 mg.mL ⁻¹)	10 minutes nebulization “classic” operating mode	68	0.68 ± 0.04 mL
Gentamicin solution (4 mL at 80 mg.mL ⁻¹)	10 minutes nebulization “sonic” operating mode	36	0.30 ± 0.02 mL

9
10

11 Table 2: Design of the drug deposition experiments conducted on the plastinated nasal cast
12 and results of the aerosol output measurements. “sonic” operating mode corresponds to
13 nebulization with 100 Hz acoustic airflow. “classic” operating mode corresponds to
14 nebulization without acoustic pressure waves.

15

Table 3

	40 mg/mL left sinus	40 mg/mL right sinus	80 mg/mL left sinus	80 mg/mL right sinus	40 mg/mL left sinus acoustic airflow	40 mg/mL right sinus acoustic airflow	80 mg/mL left sinus acoustic airflow
40 mg/mL - right sinus	p = 0.679						
80 mg/mL - left sinus	* p < 0.0001						
80 mg/mL - right sinus		* p < 0.0001	* p = 0.005				
40 mg/mL - left sinus acoustic airflow	* p < 0.0001						
40 mg/mL - right sinus acoustic airflow		* p < 0.0001			p = 0.242		
80 mg/mL - left sinus acoustic airflow			* p = 0.0005		* p < 0.0001		
80 mg/mL - right sinus acoustic airflow				* p = 0.002		* p = 0.001	* p = 0.019

19
20
21
22
23
24

Table 3: Statistical analysis of gentamicin aerosol deposition into the maxillary sinuses of the plastinated nasal cast. Light grey: impact of a 100 Hz acoustic airflow; grey: impact of the initial gentamicin concentration introduced into the nebulizer, dark grey: impact of endonasal anatomical features (disparate size and morphology of left and right ostia).